Face-Centered Cubic Supra-Crystals and Disordered Three-Dimensional Assemblies of 7.5 nm Cobalt Nanocrystals: Influence of the Mesoscopic Ordering on the Magnetic Properties

I. Lisiecki, D. Parker, C. Salzemann, and M. P. Pileni*

Laboratoire LM2N, UMR CNRS 7070, Université Pierre et Marie Curie, bât. F, B.P.52, 4 place Jussieu, F-752 31 Paris Cedex 05, France

Received March 6, 2007. Revised Manuscript Received May 4, 2007

Previously, we have shown that we can control the mesoscopic order in three-dimensional (3D) assemblies of 7.5 nm Co nanocrystals to give either face-centered cubic (fcc) supra-crystals or disordered aggregates. These 3D assemblies provide an intermediate between the atomic and the bulk state and have the potential to exhibit many interesting new properties. In this paper we compare the magnetic properties of well-characterized disordered and fcc ordered 3D assemblies and find that there are significant differences arising from the mesoscopic order. We propose that this is due to the difference in anisotropy and distribution of dipolar interaction energies in the two systems and that this represents a new intrinsic property of magnetic supra-crystals.

I. Introduction

Over the last 10 years the self-assembly of nanocrystals deposited on substrates by evaporation of colloidal solutions has been intensively investigated.[1−5] One of the most important parameters needed to achieve self-assembly of nanocrystals into long range ordered arrays is a narrow particle size distribution.[4,6] More recently, the preparation of well ordered multi-dimensional structures, from metallic, semiconductor, and magnetic nanocrystals with a low size dispersion, is becoming increasingly important. Indeed, as a result of the periodic ordering of the nanocrystals, such 3D superlattices exhibit unique transport,[7] optical,[8] and structural[9] collective properties. For example, it is well-known that color in precious opal results from the high ordering of the uniform silica spheres.[10] Enhanced mechanical stability of columns made of cobalt nanocrystals has been shown to arise from the face-centered cubic (fcc) supra-structure.[9] A year ago, vibrational coherence in Raman scattering was observed in supra-crystals made of silver nanocrystals.[11] At the same time, another group gave evidence of the effect of ordering in 3D CdSe assemblies by observing changes in the photoluminescence properties between ordered and disordered assemblies.[12]

Magnetic nanocrystals have attracted much interest in recent years as they have many potential technological applications, the most significant being in high-density data storage.[13] They are also of great interest on a fundamental level as analogies can be drawn between atomic scale magnetic systems and mesoscopic scale magnetic nanocrystal systems. As observed by Néel, dilute assemblies of magnetic nanocrystals exhibit superparamagnetic behavior as seen in systems where magnetic atoms are diluted in a nonmagnetic matrix. In more concentrated magnetic nanocrystal systems, dipole−dipole interactions are induced which have a significant effect on the magnetic behavior. For highly concentrated dispersions it has been shown these interactions lead to spin-glass-like behavior as observed in systems where magnetic atoms interact via long-range RKKY interactions.[14−16]

In 2003, Lisiecki et al. made, for the first time, fcc supra crystals constructed of cobalt nanocrystals by slow evaporation of a colloidal solution on a highly oriented pyrolitic graphite (HOPG) substrate.[4] More recently, new synthetic and deposition procedures have been developed, enabling the fabrication, with the same cobalt nanocrystals, of either disordered or long range ordered three-dimensional (3D) assemblies.[17]

Various studies have been carried out to compare the magnetic properties of nanocrystals arranged in 3D as-

(1) Pileni, M. P. *J. Phys. Chem. B* **2001**, *105*, 3358−3371.
(2) Motte, L.; Billoudet, F.; Pileni, M. P. *J. Phys. Chem.* **1995**, *99*, 16425−16429. Motte, L.; Pileni, M. P. *J. Phys. Chem. B* **1998**, *102*, 4104−4109.
(3) Murray, C. B.; Kagan, C. R.; Bawendi, M. G. *Science* **1995**, *270*, 1335−1338.
(4) Lisiecki, I.; Albouy, P. A.; Pileni, M. P. *Adv. Mater.* **2003**, *15*, 712−716.
(5) *Nanocrystals forming mesoscopic structures*; Pileni, M. P., Ed.; Wiley-VCH: New York, 2005; p 251.
(6) Lisiecki, I.; Pileni, M. P. *Langmuir* **2003**, *19*, 9486−9489.
(7) Taleb, A.; Silly, F.; Gusev, A. O.; Charra, F.; Pileni, M. P. *Adv. Mater.* **2000**, *12*, 633−637.
(8) Taleb, A.; Petit, C.; Pileni, M. P. *J. Phys. Chem. B* **1998**, *10*, 2214−2220.
(9) Germain, V.; Pileni, M. P. *Adv. Mater.* **2005**, *17*, 1424−1429.
(10) Sanders, J. V. *Nature* **1964**, *204*, 1151.
(11) Courty, A.; Merme, A.; Albouy, P. A.; Duval, E.; Pileni, M. P. *Nat. Mater.* **2005**, *4*, 395−398.
(12) Zaitseva, N.; Dai, Z. R.; Leon, F. R.; Krol, D. *J. Am. Chem. Soc.* **2005**, *12*, 10221−10226.
(13) Terris, B. D.; Thomson, T. *J. Phys. D: Appl. Phys.* **2005**, *38*, R199−R222.
(14) Dormann, J. L.; Fiorani, D.; Tronc, E. *Adv. Chem. Phys.* **1997**, *98*, 283−294.
(15) Jonsson, P.; Hansen, M. F.; Svedlindh, P.; Nordblad, P. *J. Magn. Magn. Mater.* **2001**, *226*, 1315−1316.
(16) Parker, D.; Ladieu, F.; Vincent, E.; Mériguet, G.; Dubois, E.; Dupuis, V.; Perzynski, R. *J. Appl. Phys.* **2005**, *97*, 10A502.
(17) Lisiecki, I.; Albouy, P. A.; Pileni, M. P. *J. Phys. Chem. B* **2004**, *108*, 20050−20055.

10.1021/cm070625x CCC: $37.00
Published on Web 07/17/2007

semblies with those in two-dimensional (2D) arrays or powder form.[18−21] Effects such as slower magnetic relaxation[18,19] and increased coercivity and remanence[21] in the 3D assemblies were attributed to the increase in dipolar interaction. A computational study by Kechrakos and Trohidou compared 3D assemblies with square cubic (sc) and fcc symmetry.[22] Their study predicted some differences arising from the change in structure such as an increase in the magnetization and coercivity for the fcc compared to the sc lattice. To date, we are not aware of any theoretical or experimental study which has shown clearly that differences in magnetic properties can arise when nanocrystals are arranged in an ordered 3D lattice compared to a disordered assembly.

Here we report a comparative study of 3D ordered and disordered assemblies of 7.5 nm cobalt nanocrystals. Using the ability we have to control the mesoscopic order, we have prepared disordered and highly ordered fcc supra-crystal assemblies from the same nanocrystals. A carefully controlled study has been made to clearly show the effect of order on the magnetic properties.

II. Experimental Section

II. A. Products. All materials were used without further purification. Cobalt acetate and lauric acid are from Aldrich; isooctane, hexane, and sodium di(ethylhexyl) sulfosuccinate (Na(AOT)) are from Fluka; sodium borohydride is from Acros. The synthesis of cobalt(II) bis(2-ethylhexyl)sulfosuccinate ($Co(AOT)_2$) has been described previously.[23]

II. B. Equipment. Transmission electron microscopy (TEM) was performed with a Jeol JEM-1011 microscope.

Scaning electron microscopy was performed with a JMS-5510LV instrument.

Grazing incidence small-angle X-ray scattering (GISAXS) experiments were performed with a rotating anode generator operated with a small-size focus (copper anode; focus size 0.2 mm $\times$ 0.2 mm; 50 kV, 30 mA). The optics consisted of a two parabolic multilayer graded mirror in K_B geometry providing a parallel monochromatic beam. The sample was mounted on a rotation stage, and the diffraction patterns were recorded on photostimulable imaging plates. Vacuum pipes are inserted between the sample and the imaging plate to reduce air scattering. The magnetic measurements were made with a commercial SQUID magnetometer (Cryogenic S600).

II. C. Synthesis of Cobalt Nanocrystals. The synthesis of cobalt nanocrystals coated with lauric acid is described in ref 6. Reverse micelles of 5×10^{-2} M $Co(AOT)_2$ form an isotropic phase. The amount of water added in solution is fixed to reach a water concentration defined as $w = [H_2O]/[AOT] = 32$. Sodium borohydride, $NaBH_4$, added to the micellar solution reduces the cobalt ions. The sodium borohydride content is defined as $R = [NaBH_4]/[Co(AOT)_2] = 6$. Immediately after $NaBH_4$ addition, the micellar solution color changes from pink to black, indicating the formation of colloidal cobalt particles. The nanocrystals are coated with dodecanoic acid and extracted from the surfactant before being dispersed in hexane. To eliminate the largest particle size formed, the solution is centrifuged, and only the upper phase containing the smallest particles is collected.

II. D. Sample Preparation. After synthesis, the concentration of nanocrystals dispersed in hexane is fixed at 5.5×10^{-7} M. For the 2D superlattices, a few drops are deposited on an HOPG grid for TEM analysis. In order to prepare the HOPG grids a sheet of HOPG is stuck on an untreated copper grid. The HOPG is then cleaved to give a very thin layer, permitting TEM observations. To prepare the 3D assemblies, HOPG substrates (10×5 mm) are horizontally immersed in 200 μL of the colloidal nanocrystal solution. The evaporation of the solvent takes place in a nitrogen atmosphere to prevent oxidation. The temperature and atmospheric conditions are controlled to give either disordered or ordered assemblies.

(a) To form the disordered assembly, the solvent evaporation takes place at 7 °C under a nitrogen flow saturated with hexane. The evaporation time is approximately 12 h.

(b) To form the ordered assembly, the solvent evaporation takes place at room temperature under nitrogen. This is carried out in an almost completely isolated system saturated with hexane such that evaporation takes in total approximately 72 h.

II. E. Magnetization Measurements. The zero field cooled (ZFC) magnetization versus temperature is measured by cooling the sample in zero applied field from 300 to 5 K, applying a field of 20 Oe and then measuring the magnetization as the sample is heated. To measure the field cooled (FC) magnetization versus temperature, a field of 20 Oe is applied at 300 K before cooling the sample to 5 K and subsequently measuring the magnetization from 5 to 300 K. The magnetization versus field measurements are carried out at 5 K after zero field cooling of the sample. All magnetic measurements were performed with the applied field parallel to the substrate.

III. Results

To characterize the Co nanocrystals, we first investigate by TEM the 2D superlattices (Figure 1A). As we can see, these cobalt nanocrystals self-organize in a 2D hexagonal network over a long range. The size histogram of these nanocrystals, made on around 600 nanocrystals, shows that they are characterized by a mean diameter of 7.5 nm and a low size dispersion of 9.4% (Figure 1B). A profile plot made on 30 cobalt nanocrystals aligned in one direction of the hexagonal network (as marked "a" in Figure 1A) is presented in Figure 1C. The maxima of the profile correspond to the maximum contrast (i.e., the center of the nanocrystals) and the minima to the substrate (i.e., between the nanocrystals). As we can see, the profile plot exhibits sharp oscillations as a result of a good contrast of the nanocrystals relative to the substrate and their well-defined borders. The distances between 2 successive maxima are constant over a total distance of at least 300 nm, confirming the regular organization of the nanocrystals. From this we can deduce a center-to-center distance (D_{c-c}) equal to 10.3 nm. We find a mean diameter of the nanocrystals along this direction of 7.8 nm, which is the same within error as found from the histogram analysis. From these values, an interparticle gap (D_{ip}) of 2.5 nm is deduced. In addition, as we can see clearly in Figure 1D, the nanocrystals can also organize in a 3D assembly.

(18) Luis, F.; Petroff, F.; Torres, J. M.; Garcia, L. M.; Bartolomé, J.; Carrey, J.; Vaurès, A. *Phys. Rev. Lett.* **2002**, *88*, 217205−217209.
(19) Sachan, M.; Walrath, N. D.; Majetich, S. A.; Krycka, K.; Kao, C.-C. *J. Appl. Phys.* **2006**, *99*, 08C302.
(20) Farrell, D.; Ding, Y.; Majetich, S. A.; Sanchez-Hanke, C.; Kao, C.-C. *J. Appl. Phys.* **2004**, *95*, 6636−6638.
(21) Yang, H. T.; Shen, C. M.; Su, Y. K.; Yang, T. Z.; Gao, H. J.; Wang, Y. G. *Appl. Phys. Lett.* **2003**, *82*, 4729−4731.
(22) Kechrakos, D.; Trohidou, K. N. *Phys. Rev. B* **1998**, *58*, 12169−12177.
(23) Petit, C.; Lixon, P.; Pileni, M. P. *Langmuir* **1991**, *7*, 2620−2625.

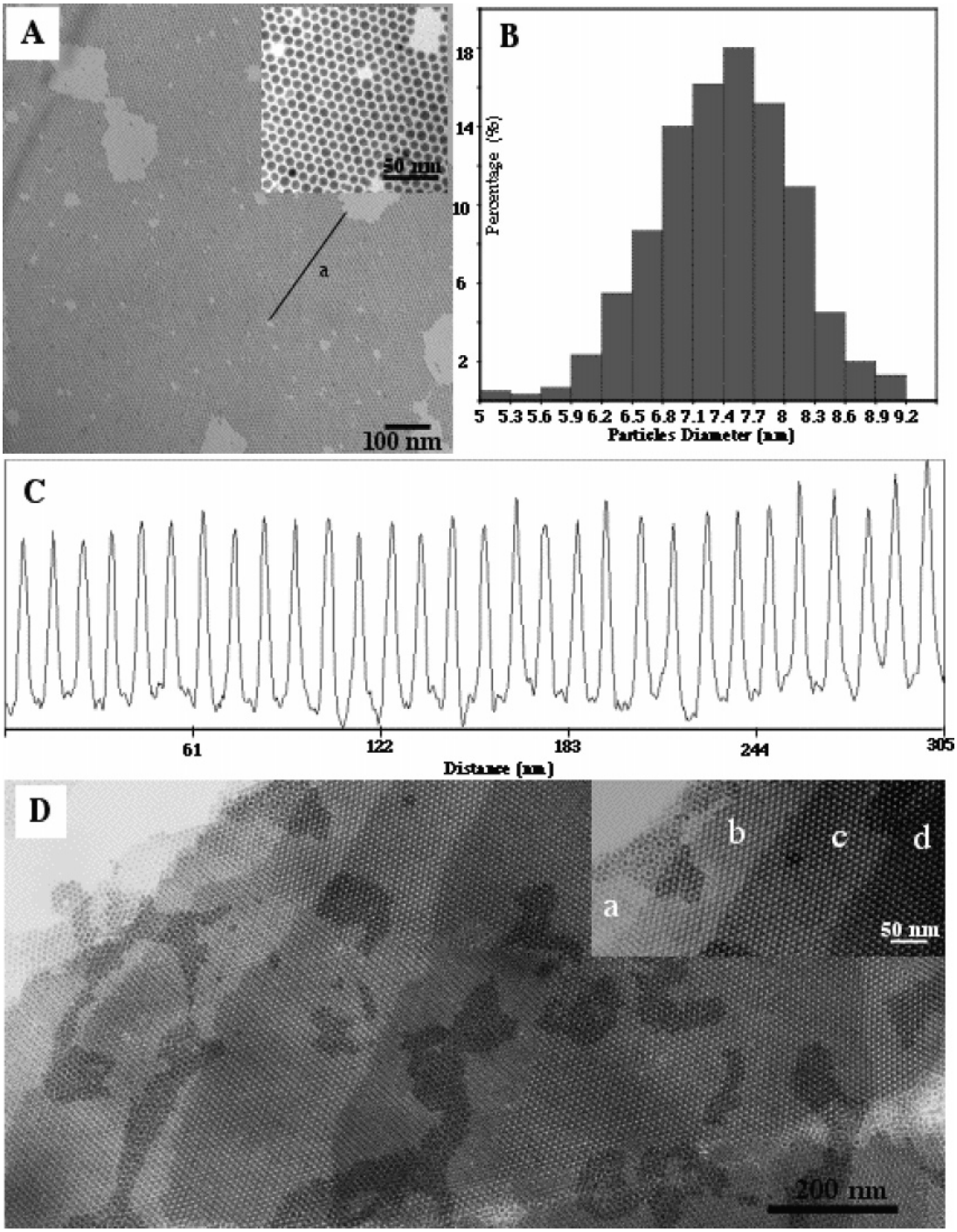

Figure 1. (A) TEM images of 7.5 nm cobalt nanocrystals ordered in a compact hexagonal monolayer and (B) the corresponding size distribution. (C) Plot profile made on nanoparticles aligned in one direction of the hexagonal network. (D) TEM image of thin 3D organizations.

The steps show the formation of 3D assemblies from one layer (a) to a multilayer system (b−d), thin enough to be observed by TEM. On such 3D systems it is not easy to make a profile plot however, very regular organizations are observed, whatever the number of layers (see inset in Figure 1D). A previous work using high-resolution TEM[6] has shown that the cobalt nanocrystals have a poorly crystallized fcc structure.

Figure 2A,B shows the scanning electron microscopy (SEM) images of the disordered and ordered 3D assemblies. The disordered 3D assembly is characterized by a thin film morphology (less than 500 nm) with a smooth surface (Figure 2A). For the ordered assembly different morphologies of the 3D assemblies are observed depending on the film thickness (Figure 2B). At the center of the substrate, domains characterized by a thickness of several micrometers are observed (i.e., several hundred Co nanocrystal layers). In this thicker region, the film is cracked to give blocks of random size and shape (Figure 2B). Conversely, at the borders of the sample, a step-like uncracked surface is observed corresponding to areas with a thickness of less than 1 μm (inset, Figure 2B). For both samples, at low magnification (not presented here) it appears that the deposition is not homogeneous on the substrate.

Figure 2C,D show the corresponding GISAXS diffraction signatures of the disordered and ordered samples, respec-

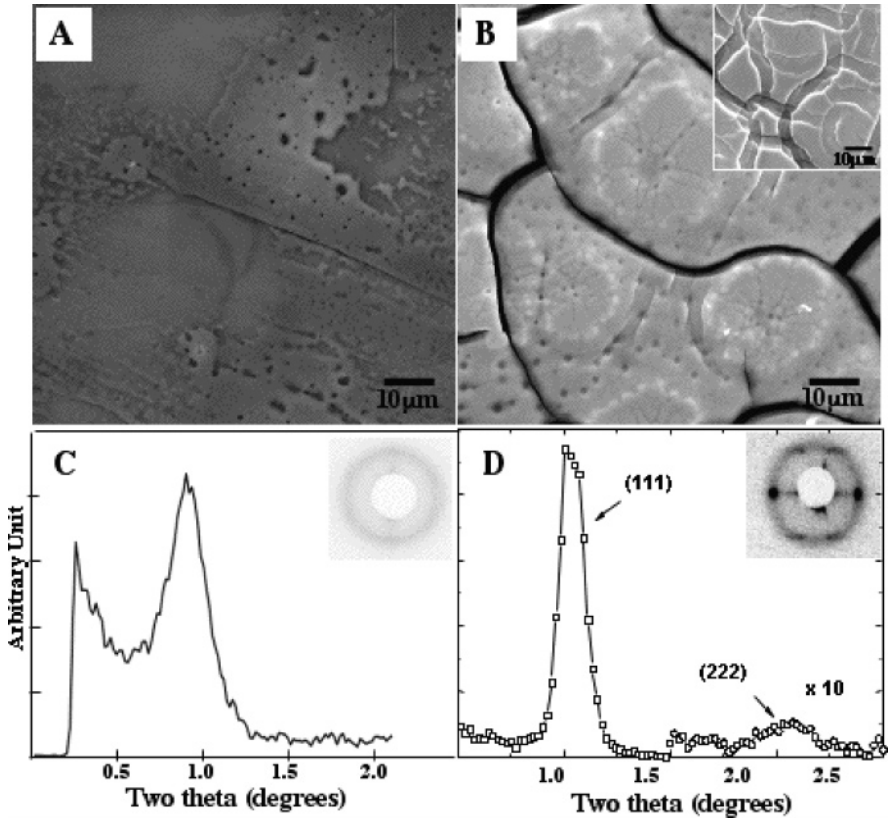

Figure 2. SEM image of (A) disordered 3D assemblies of 7.5 nm Co nanoparticles and (B) the ordered sample in the thicker region. Inset: the same supra-crystal in the thinner region. GISAXS diffractograms corresponding to the disordered (C) and ordered (D) samples. Insets: corresponding small-angle X-ray diffraction patterns obtained in a grazing incidence geometry.

Table 1. Structural and Magnetic Parameters Extracted from the GISAXS Patterns, the ZFC Magnetization Curves, and the Hysteresis[a]

	ordered	disordered
(111) stacking periodicity (nm)	8.6 ± 0.1	9.4 ± 0.1
$\delta q_{1/2}$ (nm^{-1})	0.050	0.260
D_{c-c} (nm)	10.5 ± 0.1	11.5 ± 0.1
D_{i-p} (nm)	3.0 ± 0.5	4.0 ± 0.5
T_B (K)	112 ± 3	120 ± 6
M_r/M_s	0.53 ± 0.2	0.54 ± 0.2
H_c (Oe)	900 ± 50	600 ± 50

[a] $\delta q_{1/2}$, the half width at half-maximum; D_{c-c}, center-to-center nanocrystal distance; D_{i-p}, border-to-border distance of nanocrystals considering a nanocrystal size of 7.5 nm; T_B, blocking temperature; M_s, saturation magnetization; M_{snat}/M_{sann}, ratio of native M_s to annealed M_s; and H_c, coercivity.

tively. The diffraction pattern (inset, Figure 2C) of the disordered sample shows a diffuse ring suggesting the absence of any long-range ordering. This is further confirmed by the $\theta-2\theta$ diffractogram which shows a low-intensity peak characterized by a markedly broad half-width at half-maximum ($\delta q_{1/2}$) of 0.260 (see Table 1). From the diffuse ring distance, we find a periodicity of 9.4 nm. As shown in ref 17, by assuming an fcc local packing in the disordered system, a D_{c-c} value equal to 11.5 nm is found, which leads to an interparticle gap equal to 4.0 nm. The GISAXS pattern of the ordered sample displays several reflections, all typical of an fcc structure.[4] The corresponding diffractogram shows a thin, intense Bragg peak corresponding to the first order of the (111) reflection, and the second-order reflection is also observed (Figure 2D). The (111) reflection corresponds to the stacking planes parallel to the substrate. The first-order peak is very narrow and nearly resolution-limited (i.e., 0.050 nm^{-1}) indicating a long-range ordering. From the position of the (111) peak, we find a stacking periodicity equal to 8.6 nm from which we deduce a D_{c-c} equal to 10.5 nm and an interparticle gap of 3.0 nm.

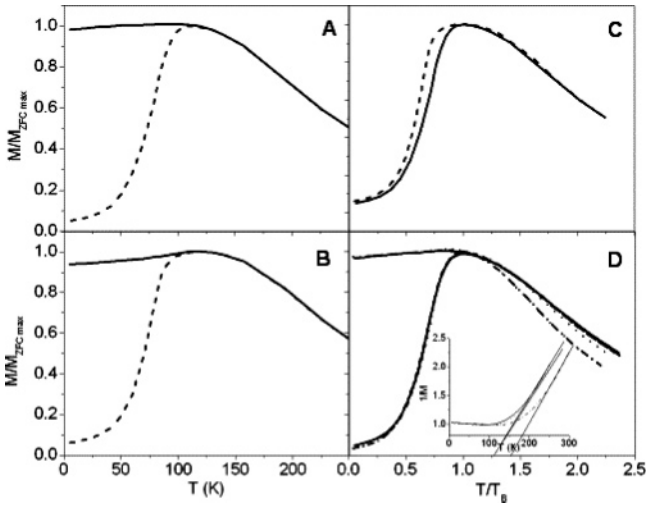

Figure 3. (A) FC (solid line) and ZFC (dashed line) magnetization versus temperature curves of a supracrystal assembly; (B) FC (solid line) and ZFC (dashed line) magnetization versus temperature curves of a disordered 3D assembly; (C) zero field magnetization versus temperature curves normalized to T_B of a supra-crystal (solid line) and a disordered (dashed line) 3D assembly; and (D) FC and ZFC magnetization versus temperature curves supracrystal assemblies made from Co nanocrystals from synthesis 1 (solid line and dashed line), synthesis 2 (dotted line), and synthesis 3 (dotted-dashed line).

Figure 3A shows the FC and ZFC magnetization versus temperature curves for an fcc ordered (supra-crystal) assembly of Co nanocrystals.[24] In the ZFC measurement the

sample has been cooled in zero field; hence, there is no net alignment of the spins at 5 K, and the magnetization is close to zero. As the temperature is increased, the spins become progressively "unblocked", aligning toward the field direction and the magnetization increases until it reaches a maximum which we use to define the blocking temperature, T_B. Above T_B the behavior is paramagnetic; that is, the thermal energy increases to such an extent that the increased dynamic rotation of the spins prevents alignment in the field direction and the magnetization decreases with increasing temperature. In the FC curve the magnetization remains nearly constant from 5 K to T_B. Above T_B the behavior is paramagnetic and the magnetization decreases with increasing temperature in line with the ZFC curve.

To check the consistency of the magnetic behavior of the supra-crystal samples, several assemblies were made from different synthesis batches of Co nanocrystals. The ZFC/FC curves for these samples, normalized to T_B, are shown in Figure 3D. Two supra-crystal samples are prepared with nanocrystals from synthesis 1, and we see that the ZFC/FC curves of these samples are perfectly superimposed, indicating good reproducibility of the supra-crystal assembly technique. The T_B of these two samples was 106 ± 3 K. The supra-crystal prepared from nanocrystals from synthesis 2 had a slightly higher T_B (112 ± 3 K), and we see that above T_B (i.e., in the paramagnetic region) the slope of the M versus T curve is slightly steeper. A third synthesis gave a supra-crystal with a significantly elevated T_B (136 ± 3 K), and here we see that the slope in the paramagnetic region is increased further. We attribute these variations in T_B to the slight variation in nanocrystal volume from one synthesis batch to another. Size changes within the error bounds of nanocrystal volume determined by TEM (i.e., ±0.5 nm) could account for the observed changes in T_B. It was shown in ref 25 that a change in diameter of 1 nm could account for a change in T_B of 43 K.

We point out that, despite these variations in T_B from one synthesis batch to another, the normalized FC and ZFC curves for all ordered samples are perfectly superimposed below T_B. The inset of Figure 3D shows a plot of $1/M$ of the FC curves versus T. Fitting the paramagnetic region using the Curie−Weiss law gives a θ value of 140 K for the assemblies from syntheses 1 and 2 and 180 K for synthesis 3. The derived Curie−Weiss temperature is larger for the samples with a higher T_B; this is consistent with an increased nanocrystal size leading to an increased interparticle interaction.

To study the effect of order on the magnetic properties, FC and ZFC magnetization versus temperature curves are measured for a number of "pairs" of ordered and disordered samples to check the consistency of our results. The "same" nanocrystals are used for both samples to eliminate any influence of nanocrystal size or size distribution on the magnetic properties. Figure 3A,B shows the FC/ZFC curves

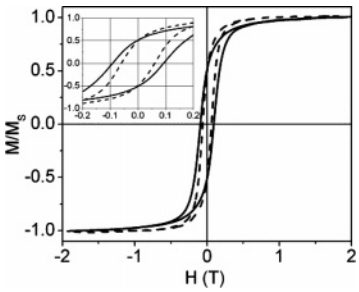

Figure 4. Magnetization versus field curves at 5 K, normalized to M_s of a supracrystal (solid line) and disordered (dashed line) 3D assembly. Inset: Magnification of the low field region.

for the supra-crystal and disordered samples, respectively. We find T_B values of 112 ± 3 and 120 ± 6 K, respectively for the ordered and disordered assemblies. The peak in the ZFC curve is significantly broader for the disordered sample compared to that of the supra-crystal sample, and this leads to the increase in the error in determining T_B. It was found that the T_B of the disordered and supra-crystal samples were always the same within the error limits with the ordered sample having a T_B sometimes slightly above and sometimes slightly below that of the disordered sample. However, the width of the ZFC peak below T_B was *always* narrower for the supra-crystal sample compared to the disordered sample. This can be seen clearly in Figure 3C where the ZFC curves of the ordered and disordered samples are normalized to T_B. Although this feature is relatively subtle, we stress that we found it to be highly reproducible within our carefully controlled comparative study.

Figure 4 shows the magnetization versus field curves for the ordered and disordered 3D Co nanocrystal assemblies. We observe that for the supra-crystal sample, the approach to saturation is more gradual than for the disordered sample and that there is a relative increase in coercive field (H_c) of 300 Oe. There is no significant difference in M_r/M_S between the ordered and disordered samples (0.53 and 0.54, respectively).

IV. Discussion

The 2D and 3D superlattices of cobalt nanocrystals coated with dodecanoic acid chains are highly stable. Samples exposed to air for a period of several weeks do not appear to oxidize as confirmed by electronic diffraction for the 2D assemblies and magnetization measurements for 3D. However, we cannot exclude the possibility of a very thin layer of oxide (probably CoO), which would not be detectable by electronic diffraction techniques. Advanced oxidation (more than 1 nm in thickness) gives rise to a low temperature (≈8 K) peak in the ZFC magnetization versus temperature curve.[26] We have not observed this and therefore we conclude that any oxidation present is not sufficient to modify the magnetic properties. Neither do we observe any coalescence of Co nanocrystals with time. This high stability is most likely due to the presence of the dodecanoic acid chains

(24) In a previous paper (ref 17) concerning the first formation of ordered and disordered 3D assemblies some preliminary magnetic results were published which are not coherent with those reported here. We have since discovered that this was due to sample mismatch in our first publication.

(25) Tracy, J. B.; Weiss, D. N.; Dinega, D. P.; Bawendi, M. G. *Phys. Rev. B* **2005**, *72*, 064404−064411.
(26) Wang, Z. L.; Harnfenist, S. A.; Whetten, R. L.; Bentley, J.; Evans, N. D. *J. Phys. Chem. B* **1998**, *102*, 3068−3072.

protecting the nanocrystal surface. This coating strongly attaches to the metallic nanocrystal by a covalent bond between the Co surface and the O atom of the acid group. The organic chains are also responsible for the long-range superlattices. It has been reported that, at room temperature, the alkyl chains assemble into groups with a preferential parallel intermolecular orientation (i.e., all-trans arrangement) forming pillars or bundles on the facets of the metal nanocrystal.[26,27] These bundles interdigitate giving long-range order and high stability of the superlattices. In our 2D superlattices, if we take into account the alkyl chain lengths (≈1.78 nm) and the Co−O covalent bond distance (≈0.21 nm), the interparticle distance is about 2.5 nm, which indicates a mean chain interdigitation of 1.5 nm (nine C−C distances).

In the case of the supra-crystals, the interparticle gap found is equal to 3.0 nm, which implies a mean chain interdigitation of 1.0 nm (around six C−C bonds). We propose that this decrease in interdigitation in 3D could be due to some remaining solvent molecules (hexane), which have become trapped between the nanocrystals and hinder the interdigitation of the chains. In the case of the monolayer, we assume that these molecules will be easily evaporated.

From the same nanocrystals we are able to form either disordered or long-range ordered fcc supra-crystals. The fact that we have the same building blocks enables a rigorous comparative structural investigation. The disordered sample shows no reflections in the GISAXS pattern; however, the diffractogram reveals a (111) peak, although very broad and weak, indicating a local ordering. As the supra-crystal clearly shows an fcc mesostructure we extend this to the case of the disordered sample and hence deduce a periodicity from an fcc stacking. The resulting interparticle gap is equal to 4.0 nm, that is, 1.0 nm higher than is found for the supra-crystal. This is to be expected as the disordered structure must necessarily be less dense than the highly compact fcc structure of the supra-crystal. The GISAXS study clearly indicates a higher coherence length of the fcc crystallized domain compared to the disordered sample. Therefore, the structural environment of the Co nanocrystals in the supra-crystal is considerably more uniform than in the disordered sample.

The magnetization versus temperature measurements show that both the supra-crystal and the disordered samples have a T_B of around 100 K; this is a significantly higher value than has previously been observed for dilute systems of Co nanocrystals of a similar size[28] and therefore indicates that there are strong dipolar interactions between the nanocrystals. This is also supported by the flat FC curve below T_B which is typical of interacting nanoparticle systems. The ZFC peak width is dependent on the distribution of barrier energies in the system, with a larger distribution giving a broader peak. The barrier energy (E_b) is the sum of the anisotropy energy, $E_a = k_a V$ (where k_a is the anisotropy constant and V is the nanocrystal volume), and the interparticle dipole interaction energy, E_{dd}. In fact, it has been shown that there is a significant contribution of the surface anisotropy to E_a;[29] however, this does not affect our discussion. As the nanocrystals used to form the two assemblies are the same we can discount any effects of nanocrystal volume distribution and anisotropy. The observed effect must therefore arise from the mesoscopic order of the nanocrystals in the assembly. As pointed out in ref 22, the dipolar interactions are highly directionally sensitive, and hence the nanocrystal geometrical environment is expected to play a significant role. In the supra-crystal sample, GISAXS measurements show that there is fcc ordering with a long coherence length. Within each fcc domain we can consider that the Co nanocrystal environment is very uniform, that is, that each nanocrystal has the same geometrical coordination and that the nanocrystal spacing is regular. This will lead to a low distribution of E_{dd} and hence E_b within each fcc domain. The disordered 3D assembly has no long-range order observable by GISAXS, and we therefore conclude that the sample consists of a mixture of very short-range ordered fcc domains and amorphous regions. Consequently the nanocrystals in this array will have a much less uniform geometrical arrangement than in the ordered array. This leads to a greater distribution of E_{dd} and in turn E_b compared to the supra-crystal sample and gives the observed broadening of the ZFC peak for the disordered sample.

The high field measurements also show an effect of order, namely, a higher H_c and a slower approach to saturation in the ordered sample. The difference in approach to saturation can be explained by considering the model of amorphous ferromagnets proposed by Chudnovsky and Serota.[30−32] In this model there is only short-range structural order, which leads to a local random anisotropy with a short-range correlation length. The randomness of this local anisotropy leads to a very small uniform anisotropy in the sample, referred to as coherent anisotropy. The model predicts an approach to saturation in these materials given by $\Delta M \approx 1/H^{1/2}$, which has been confirmed experimentally.[33] This experimental work has been extended to disordered nanocrystallized films[34] where a $1/H^{1/2}$ approach to saturation is also observed. In addition, the authors show that increasing the anisotropy in these films leads to a deviation from $1/H^{1/2}$ behavior toward a more linear approach to saturation, which would apply in the case of a perfect uniaxial system.

In the case of our Co nanocrystal assemblies, the disordered assembly is analogous to an amorphous ferromagnet where there is only short-range structural order and the observed fast approach to saturation is consistent with the $\Delta M \approx 1/H^{1/2}$ law. The anisotropy of the Co nanocrystals themselves is the same for both systems as they are from the same synthesis; however, as in an atomic crystal, the anisotropy of the supracrystal assembly as a whole will be

(27) Pradeep, T.; Mitra, S.; Nair, A. S.; Mukhopadhyay, R. *J. Phys. Chem. B* **2004**, *108*, 7012−7020.
(28) Petit, C.; Wang, Z. L.; Pileni, M. P. *J. Phys. Chem. B* **2005**, *109*, 15309−15316.
(29) Dormann, J. L.; D'Orazio, F.; Lucari, F.; Spinu, L.; Tronc, E.; Prené, P.; Jolivet, J. P.; Fiorani, D. *Mater. Sci. Forum* **1997**, *669*, 235−238.
(30) Chudnovsky, E. M.; Serota, R. A. *J. Phys. C: Solid State Phys.* **1983**, *16*, 4181.
(31) Chudnovsky, E. M. *J. Appl. Phys.* **1988**, *10*, 5770.
(32) Chudnovsky, E. M. *J. Magn. Magn. Mater.* **1989**, *79*, 127.
(33) Filippi, J.; Amaral, V. S.; Barbara, B. *Phys. Rev. B.* **1991**, *44*, 2842.
(34) Thomas, L.; Tuaillon, J.; Perez, J. P.; Dupuis, V.; Perez, A.; Barbara, B. *J. Magn. Magn. Mater.* **1995**, *140−144*, 437.

increased because of the long-range mesoscopic order. This is supported by a slower approach to magnetic saturation as observed in refs 34 and 35 and the observed increase in H_c with respect to the disordered sample.

Both disordered and supra-crystal samples have a remanence to saturation ratio (M_r/M_s) of approximately 0.5 (see Table 1). This value is significantly higher than normally observed for isolated Co nanocrystals of a similar volume; however, it has been found that when the nanocrystals are arranged in a 2D hexagonal assembly[28] or thin 3D superlattices[21] an increase in M_r/M_s is observed. This has been attributed to an increase in dipolar interaction when the nanocrystals are organized in two dimensions.[28] Therefore, in our system, where we expect relatively strong interparticle interactions due to the 3D coordination, is not surprising that we find a high M_r/M_s.

There is a difference in sample thickness and morphology between the disordered and supra-crystal samples which could lead to some differences in magnetic behavior. However, we are confident that this is not the reason for the observed effects of order reported in this work. In another paper[35] we show that after annealing the samples there are no longer any differences in magnetic behavior between the ordered and the disordered samples. As the sample morphology does not change during annealing, this result eliminates the possibility of sample morphology playing a role in the magnetic properties of the 3D assemblies.

V. Conclusion

In this paper, we show differences in the magnetic properties of highly crystallized supra-crystal and disordered 3D assemblies of cobalt nanocrystals arising from the mesoscopic fcc ordering of Co nanocrystals. The strength of this work comes from the fact that the 3D assemblies (ordered and disordered) are made with the same population of 7.5 nm cobalt nanocrystals (i.e., same size and size distribution) and we can be sure that the observed differences are uniquely due to the mesoscopic ordering effect. For the supra-crystal we find a narrower ZFC peak in the magnetization versus temperature curve arising from a lower distribution of interaction energies compared to the disordered sample. We also find evidence of an increase in anisotropy of the ordered sample in the higher H_c and slower approach to magnetic saturation. Our study was facilitated by the high stability of the 3D assemblies against both oxidation and coalescence of their constituent Co nanocrystals. This work adds another example to the growing list of intrinsic properties arising as a result of long-range mesoscopic ordering in 3D nanocrystal assemblies.

Acknowledgment. The authors thank the European Union for supporting this work project "Growth and supra-organization of transition and noble metal nanoclusters" Contract No. NMP4-CT-2004-001594. Many thanks are also given to Dr. Eric Vincent and Dr. Pierre Bonville of DRECAM/SPEC, CEA Saclay, for the use of their SQUID magnetometer.

CM070625X

(35) Parker, D.; Lisiecki, I.; Salzemann, C.; Pileni, M. P. Submitted for publication.